IEEE Access
Multidisciplinary | Rapid Review | Open Access Journal

Received October 30, 2018, accepted November 16, 2018, date of publication December 17, 2018,
date of current version January 4, 2019.

Digital Object Identifier 10.1109/ACCESS.2018.2885248

Compact UWB Antenna With Integrated Triple Notch Bands for WBAN Applications

SRINIVAS DODDIPALLI, (Student Member, IEEE), AND ASHWIN KOTHARI, (Member, IEEE)
Department of Electronics and Communication Engineering, Visvesvaraya National Institute of Technology, Nagpur 440010, India

Corresponding author: Srinivas Doddipalli (srinivas.mre@gmail.com)

ABSTRACT A triple-notch band planar ultra-wideband (UWB) antenna is proposed for wireless body area networks (WBANs) to suppress unwanted signals of conventional narrow band communication technologies. These notch bands are WiMAX (3.3–3.8 GHz), WLAN (5.1–5.825 GHz), and *X*-band downlink satellite communication systems (7.25–7.75 GHz). A complementary split ring resonator slot and two L-shaped stubs are introduced on an elliptical-shaped radiating patch to obtain UWB coverage from 2.9 to 12 GHz with three notch bands. The overall antenna structure is fabricated on FR4 substrate with a size of 12 mm × 19 mm which provides a size reduction of more than 42% with respect to recent literature. The simulated and measured results indicate that the proposed antenna is a good candidate for WBAN applications.

INDEX TERMS Stubs, notch bands, WBAN, UWB antenna.

I. INTRODUCTION

In recent years, WBAN systems are becoming a lucrative research area because of its wide applications in the fields of medical, health monitoring, entertainment, and remote sensing systems. However, WBAN systems require high data rates with low power utilization for efficient operation [1]–[3]. UWB technology provides high data rates, low power spectral density, large bandwidth, and robustness to multipath fading. These facets help to meet the requirements of WBAN systems. UWB is an unlicensed frequency band, as declared by the Federal Communication Commission (FCC), in frequency range from 3.1–10.6 GHz [4]. The low power restriction (-44.3 dBm) of UWB systems attracts a wide range of applications in short-range communications, wearable applications [5], remote sensing [6], IoT applications [7], microwave imaging for tumour detection [8]. UWB and other existing conventional narrow band technologies are presented in Fig. 1.

UWB antenna is an essential element of UWB systems that enables wireless communication. However, it suffers from narrow band interference from WiMAX, WLAN and X band satellite communication channels. It is essential to filter these unwanted narrow band signals to improve the quality of UWB systems. These narrow band unwanted signals in UWB spectrum can be minimized with the help of band stop filters. Using of external band stop filters lead to increase the size, cost, and complexity. In comparison to other available solutions, UWB antennas with their integrated band stop filters are a better choice for interference reduction. This interference suppression is crucial to improve the quality of service in WBAN systems.

Over the past few years, various techniques have been presented to incorporate the notch bands in UWB antennas. The simplest method to obtain notch bands is etching suitable structures on patch or ground plane [9]–[20]. In [21], a cpw fed UWB antenna integrated with stub loaded meander line resonator is proposed to achieve the triple notch bands. In [22] by applying stubs and slots in the radiating patch and parasitic stubs in the ground palne, three notch bands are obtained. Another approach is the insertion of resonator structures (such as split ring resonators) to create notch bands [23]–[25]. In addition, notch bands can be obtained by embedding slots and stubs in feed line [26]. In [27], a triple notch band UWB antenna ($22mm \times 18mm$) is designed with good performance characteristics and occupies area of $396mm^2$ which is larger in size and not recommended for most of the portable wireless communication systems. Further, a significant reduction in size and cost are is insisted for portable wireless systems. Substantial cost saving is achieved by using widely available FR4 substrate material which has excellent mechanical properties. FR4 substrate has high dissipation factor (Df) than the high frequency laminates. The dissipation factor of FR4 material increases with frequency, so as frequency rises insertion loss increases and bandwidth reduces. So that, it is difficult to obtain UWB pass band with three stop bands on a compact size FR4 substrate. Wide band antenna performance

TABLE 1. Comparison of proposed antenna with existing antenna designs.

Ref. No.	Size (mm^2)	Impedance BW	Notch bands	Center frequency / BW of notch bands	Substrate	Radiation efficiency (%)
[12]	26 × 30	3 to 11 GHz	WiMAX WLAN X-band	3.3–3.6 GHz, 5.1–5.8 GHz, 7.25–7.75 GHz	FR4, ϵ_r=4.4	80
[13]	28 × 24	2.5 to 12 GHz	WiMAX WLAN X-band	3.3–3.7 GHz, 5.1–5.9 GHz, 7.25–7.85 GHz	RT/Duroid 5880, ϵ_r=2.2	NA
[16]	26 × 30	2.55 to 11 GHz	WiMAX WLAN X-band	2.74–3.54 GHz, 4.73–5.25 GHz, 5.54–6.12 GHz, 7.6–9.1 GHz	FR4, ϵ_r=4.4	95
[18]	20 × 20	2.39 to more than 18 GHz	WiMAX WLAN X-band	2.69–4.5 GHz, 5.49–6.37 GHz , 8.15–9.61 GHz	FR4, ϵ_r=4.4	NA
[19]	30 × 20	2.6 to 13.4 GHz	WiMAX WLAN X-band	3.5 GHz, 4.6 GHz, 5.5 GHz, 9.6 GHz	FR4, ϵ_r=4.5	NA
[27]	22 × 18	2.74 to more than 10.57 GHz	WiMAX WLAN X-band	3.17–3.89 GHz, 4.87–6.19 GHz, 7.3–7.86 GHz	RT/Duroid 5880, ϵ_r=2.33	91.8
[28]	20 × 20	2.49 to more than 19.4 GHz	WiMAX WLAN X-band	3.17–3.89 GHz, 4.87–6.19 GHz, 7.23–7.86 GHz	RT/Duroid 5880, ϵ_r=2.33	90
Proposed*	12 × 19	2.95 to 12 GHz	WiMAX WLAN X-band	3.3–3.8 GHz, 5.2–6.1 GHz, 7.3–8.2 GHz	FR4, ϵ_r=4.4	95

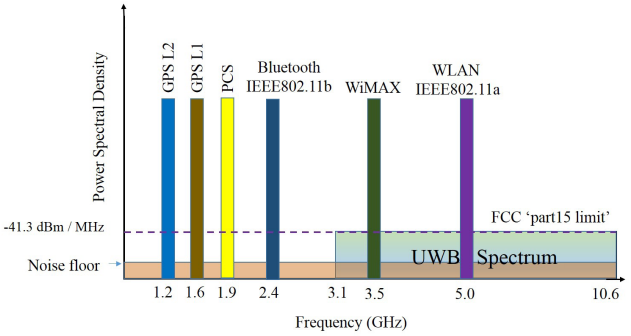

FIGURE 1. UWB and other existing conventional narrow band spectrums.

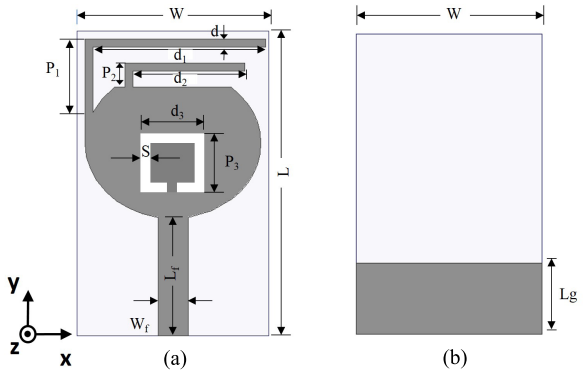

FIGURE 2. Geometrical structure of the proposed antenna. (a) Top view. (b) Bottom view.

on low cost and small size FR4 substrate material is needed to meet the requirements of portable wireless applications. Therefore, designing of UWB antennas with multiple notch bands is still an interesting and ongoing research topic due to the challenges involved in integrating the notch bands without affecting other antenna performance characteristics.

To overcome these problems, we have proposed an elliptical shaped compact planar UWB antenna with defected ground plane having dimensions $12mm \times 19mm = 228mm^2$. Two stubs are incorporated in the proposed antenna structure to realize two notch bands with improved lower operating frequency. To obtain the third notch band, a CSRR slot is etched on the patch radiator. The proposed antenna size and performance characteristics are compared with the recent literature and presented in Table 1. Due to it's compact dimensions, this antenna can be easily accommodate in WBAN systems without getting disturbance from the metallic parts of WBAN devices. Simulations of proposed antenna structure are carried out in HFSS 3D electromagnetic simulation software.

II. ANTENNA DESIGN AND ANALYSIS

The structural design of the proposed antenna with design parameters is illustrated in Fig. 2. A microstrip line with 50-ohm impedance is used to feed this antenna. The overall antenna structure is fabricated on FR4 substrate material having thickness of 1.6 mm. The fabricated prototype of this antenna is designed with compact dimensions ($12mm \times 19mm$).

The antenna is designed with a printed elliptical radiator loaded with two inverted L-shaped stubs to introduce two notch bands with improved lower operating frequency.

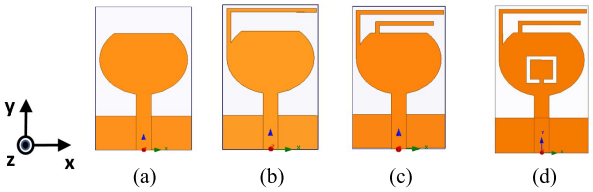

FIGURE 3. Design approach and structure modifications. (a) Basic structure. (b) With stub L_1. (c) With L_1 & L_2 stubs. (d) Proposed antenna.

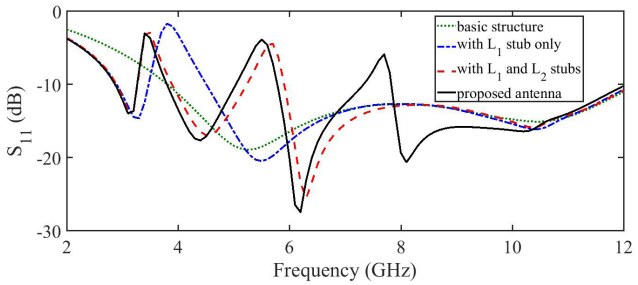

FIGURE 4. Effect of structural modifications on reflection coefficient.

Here, elliptical radiating structure is chosen to provide wide bandwidth and occupies less size than other conventional circular or rectangular radiating structures. In first step, an elliptical shaped radiator is designed with the basic elliptical antenna equations [29] and optimized it's major and minor axis dimensions to achieve improved wideband performance. The upper portion of the elliptical radiator is removed to decrease the radiator size without affecting the antenna impedance bandwidth. Stubs can be easily accommodated in small area which provide the lower operating frequency. In the proposed antenna design, embedding of two stubs to the radiating patch provides improved performance in lower operating frequency and also provides two notch bands. To obtain the third notch band a CSRR slot is etched on the patch radiator.

Fig. 3 illustrates the structural modifications of various antennas and corresponding impedance bandwidth variations are presented in Fig.4. An indicative improvement in impedance bandwidth and integration of notch bands are noticed with respect to the corresponding structural modifications. L_1 $(d_1 + P_1)$ and L_2 $(d_2 + P_2)$ are the total lengths of exterior and interior stubs respectively. Each stub length is tuned according to the corresponding notch band frequencies, i.e., approximately equal to quarter wavelength of each stubs at corresponding center frequencies [30].

The notch band frequency for the corresponding stub length can be postulated as

$$f_{notch} = \frac{C}{2 * L_{stub} * \sqrt{\epsilon_{eff}}} \tag{1}$$

$$\epsilon_{eff} = \frac{\epsilon_r + 1}{2} \tag{2}$$

Where L_{stub} is stub length at desired notch band center frequency, ϵ_{eff} is an effective dielectric constant of the substrate material.

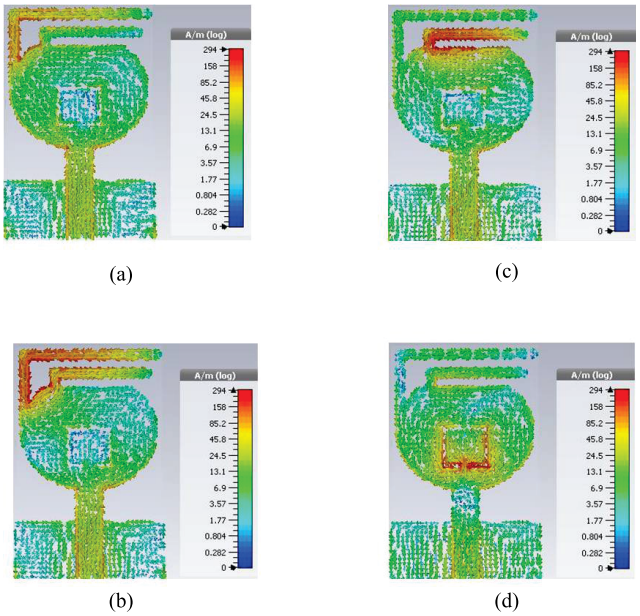

FIGURE 5. Current distributions on proposed antenna at various frequencies. (a) at 3.1 GHz. (b) at 5.5 GHz. (c) at 3.5 GHz. (d) at 7.5 GHz.

The basic structure presented in Fig. 3(a) is exhibiting impedance bandwidth from 3.85–12 GHz only. To cover the complete UWB from 3.1–10.6 GHz, an inverted L-shaped stub (L_1) is integrated as shown in Fig. 3(b). This stub increases the electrical length of the patch which helps in improving the lower operating frequency (2.9–12 GHz) and also introduces a notch band with center frequency at 3.5 GHz to filter the signals of WiMAX band. Fig. 3(c) presents the inclusion of another L-shaped stub L_2 to obtain a notch band with center frequency at 5.5 GHz to filter the signals of WLAN systems.

Fig. 3(d) shows integration of a CSRR slot on the elliptical shaped patch radiator. This CSRR slot helps to obtain the third notch band with center frequency at 7.5 GHz [7]. Total effective length of CSRR slot is denoted by L_3 $(2 * P_3 + 2 * 2 * d_3 - 3 * 0.5)$.

The notch band frequency for the corresponding dimensions of CSRR slot length can be postulated as

$$f_{notch(slot)} = \frac{C}{4 * L_{slot} * \sqrt{\epsilon_{eff}}} \tag{3}$$

Where L_{slot} is total length of CSRR slot at desired notch band center frequency.

III. ANALYSIS OF CURRENT DISTRIBUTIONS AND INPUT IMPEDANCE VARIATIONS

In Fig. 5, vector surface current distributions are reported to explain the impact of slot and stubs in introducing notch bands. Fig. 5(a) illustrates strong current distribution in stub L_1, which enhances the performance at lower operating frequency. In Fig. 5(b), the surface currents are concentrated more on L_1 stub, and the direction is opposite to the remaining

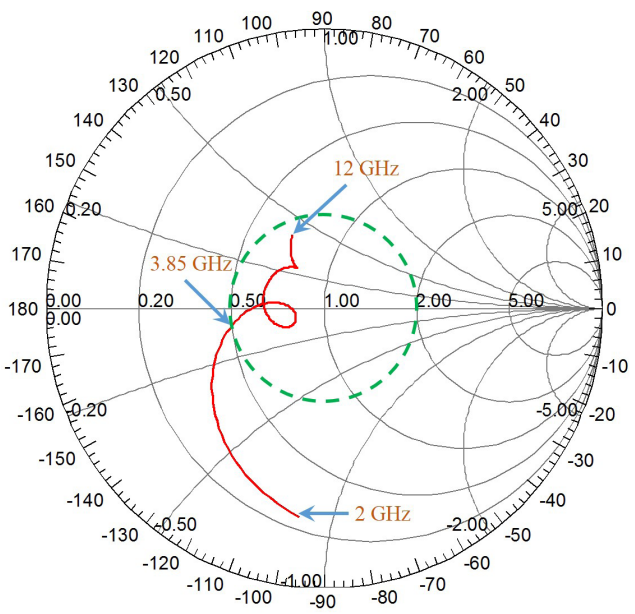

(a)

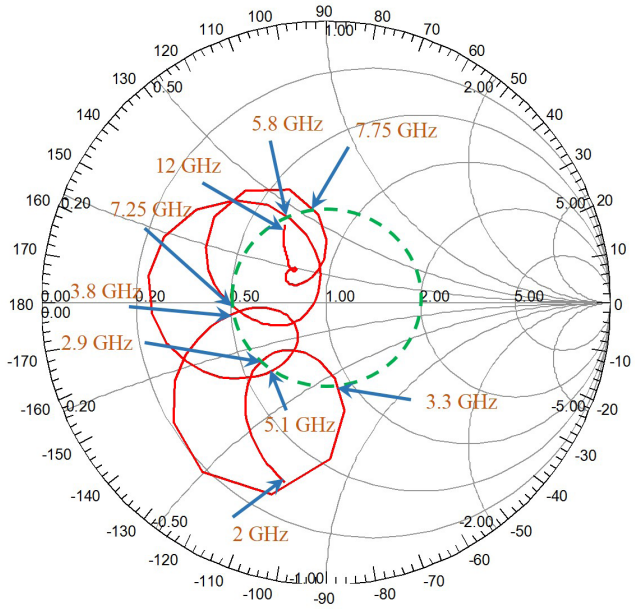

(b)

FIGURE 6. Input impedance variations on smith chart. (a) Basic antenna structure. (b) Proposed antenna structure.

patch currents that lead to a notch band at WiMAX band. The stub length is chosen equal to $\lambda_g/4$ that act as a short circuit and creates a notch band at WiMAX [26], [31]. Due to this reason the currents in patch are opposite the patch currents. Similarly, in Fig. 5(c), the surface currents are concentrated more on L_2 stub, and the direction of currents are in opposite to the patch currents that create a notch band at WLAN band. Fig. 5(d) shows strong magnitude of currents around the slot that leads to reflect maximum energy back to the input terminals which causes a notch band at X band.

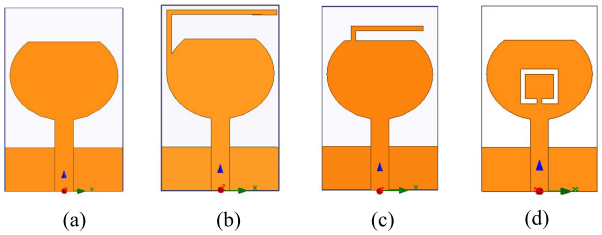

(a) (b) (c) (d)

FIGURE 7. Structural modifications for individual notch bands. (a) Basic. (b) With L_1 stub. (c) With L_2 stub. (d) With slot.

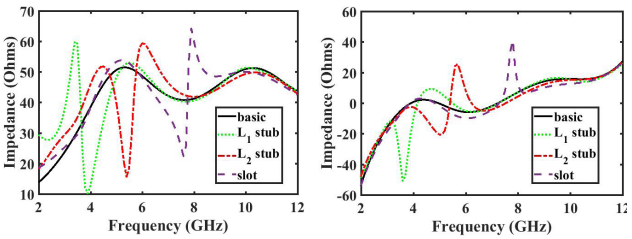

FIGURE 8. Input impedance variations with respect to structural modifications: (a) Real (b) Imaginary.

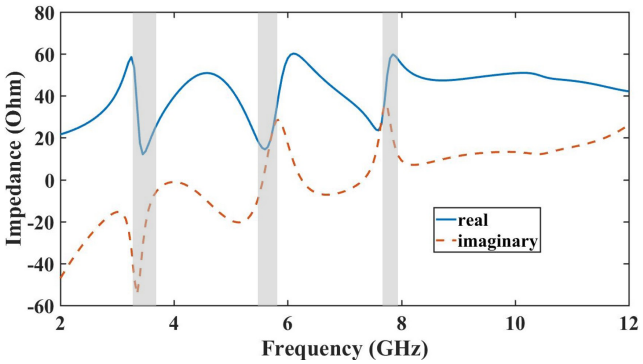

FIGURE 9. Input impedance curves of proposed antenna.

The input impedance variations can also observed from smith charts presented in Fig. 6. From the smith chart shown in Fig. 6(a), the basic antenna structure covers the impedance bandwidth from 3.85–12 GHz which does not cover entire UWB band. From the smith chart presented in Fig. 6(b), for the proposed design, clearly shows the UWB pass band from 2.9–12 GHz and three notch bands at 3.3–3.8 GHz, 5.1–5.8 GHz, and 7.25–7.75 GHz.

The antenna designs for individual notch bands and the corresponding impedance graphs are depicted in Fig. 7 and Fig. 8 respectively. From Fig. 8, imaginary impedance curves infer the series resonance behavior at 3.5 GHz and 5.5 GHz frequencies while the real impedance values being nearly equal to zero. Slot insertion in the basic antenna leads to peak real impedance which shows a parallel resonance behavior at 7.5 GHz. By merging these indiviudal designs onto a single substrate has resulted in the impedance characteristics as presented in Fig. 9. From this figure, it is clearly seen that the impedance properties shown by individual designs

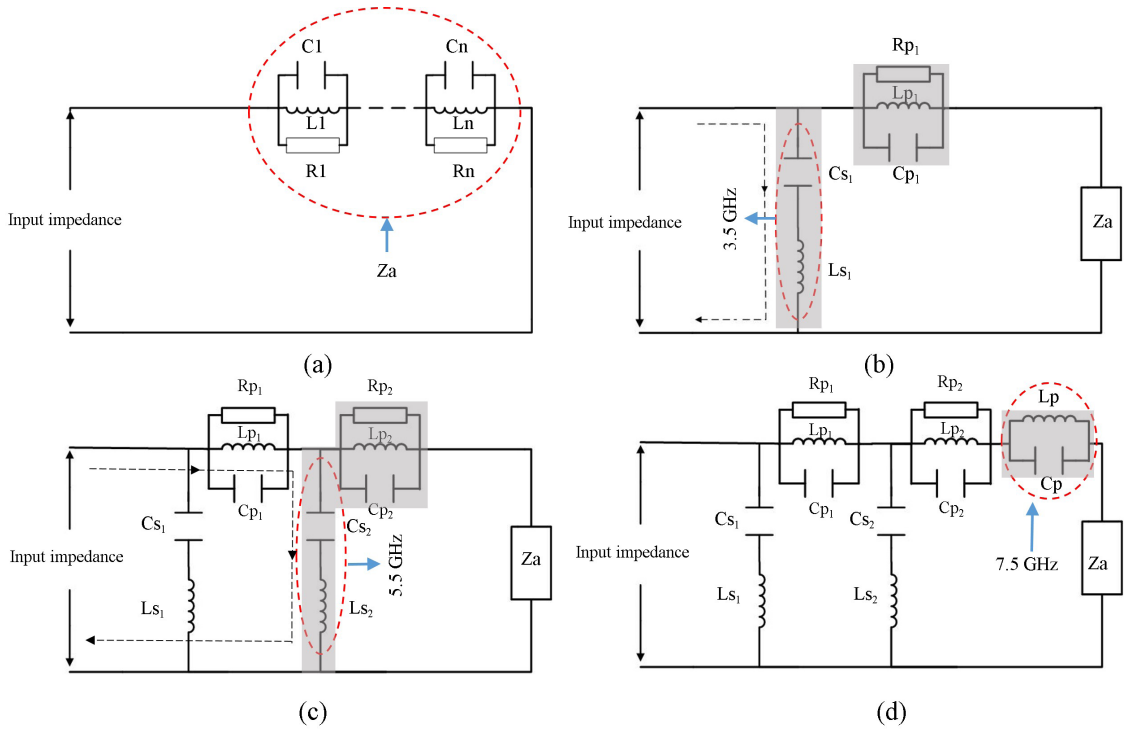

FIGURE 10. Equivalent circuit models, (a) Equivalent model for UWB antenna (b) UWB antenna with L_1 stub (c) UWB antenna with L_1 and L_2 stubs (d) proposed antenna.

are preserved at the required frequency bands. In Fig. 10, an equivalent circuit for the proposed antenna has been presented, in which the stubs and slot are represented by series and parallel resonance circuits respectively [26], [31]. In this figure, basic UWB antenna impedance is represented by '*Za*'. The stubs 'L_1 and L_2 are represented by series lumped elements Ls_1, Cs_1 and Ls_2, Cs_2 respectively. These series L and C elements act as short circuit at frequencies corresponding to the $\lambda_g/4$ length of the each stub and the maximum amount of power will return back to the input terminals of the antenna which cause to reject the frequencies at WiMAX and WLAN bands. Similarly, the CSRR slot is represented by using lumped parallel L and C elements, which cause to high impedance at frequency corresponding to the $\lambda_g/2$ length of slot as shown in Fig. 10(c). The high impedance due to the slot cause to reflect back the maximum power to the input terminals which reject the frequencies of X band (7.25–7.75 GHz).

IV. PARAMETRIC STUDY

Parametric investigation of the slot and stub lengths is performed to determine better performance of the proposed antenna. In this study, slot length and stub lengths are tuned to get corresponding notch bands at desired frequency bands.

A. EFFECT OF STUB (L_1)

Integrating a stub in proposed antenna structure has two advantages: (a) lowering the operating frequency due to increase in electrical length or current path [32], and (b) introducing a stop band [33], [34]. The L_1 stub is tuned to act as short circuit and leads to reject the frequencies corresponding to the quarter wavelength of stub. The insertion of L_1 stub leads to improvement in lower operating frequency (2.9 GHz) and also introduces a notch band from 3.3–3.8 GHz. The influence of stub length (L_1) on impedance bandwidth is illustrated in Fig. 11. With the increment of stub length from 13.5 *mm* − 15.3 *mm*, a significant down shift in notch band center frequency from 3.75 GHz to 3.55 GHz is observed. Thus, the evaluated optimal stub length of L_1 is considered to be 15.3 *mm* for a notch band at WiMAX band.

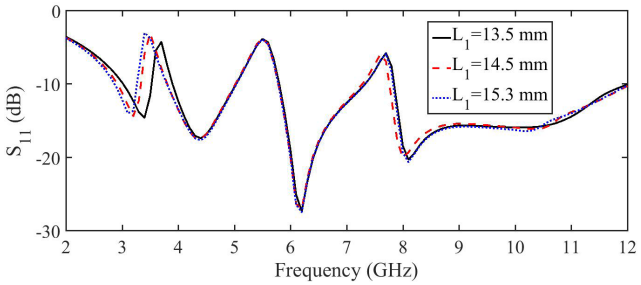

FIGURE 11. Reflection coefficient plot for different values of L_1.

B. EFFECT OF STUB (L_2)

Another inverted L-shaped stub (L_2) is embedded to the proposed antenna structure as shown in Fig. 3(c). This stub results in the creation of an additional notch band which is

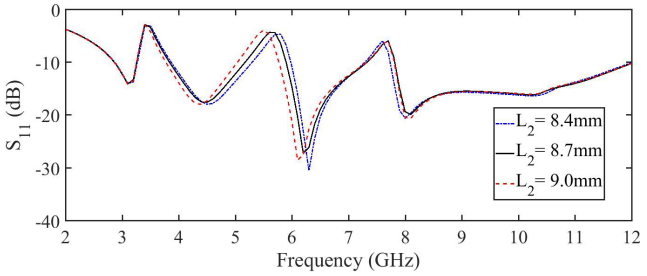

FIGURE 12. Reflection coefficient plot for different values of L_2.

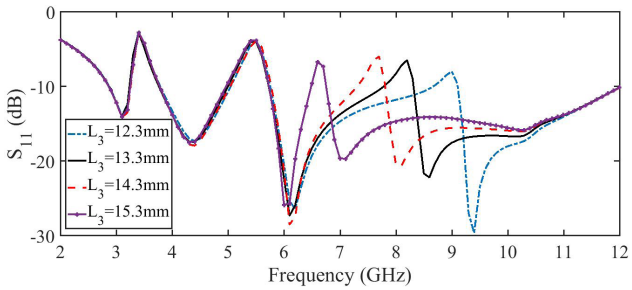

FIGURE 13. Return loss plot for different values of L_3.

intended to suppress the WLAN band (5.125–5.825 GHz). This notch band is adjusted by tuning the stub length (L_2). Stub length has been varied in the range of $8.4mm - 9.0\ mm$ which shows a considerable shift in the notch band at WLAN band and has minimal effect on the other notch bands. Thus, from the Fig. 12 the optimal value of stub length L_2 is considered to be 8.7 *mm*, as it provides a notch band at center frequency 5.5 GHz.

C. EFFECT OF SLOT LENGTH (L_3)

A CSRR slot is etched on the elliptical patch to introduce the third notch band at 7.5 GHz. This slot length has been taken as approximately equal to half guided wavelength at the corresponding notch band frequency. The return loss plot presented in Fig. 13 shows notch band variation with respect to changes in slot length. Increase in slot length shifts the notch band to lower frequency. Slot length is optimized to create a notch band at 7.5 GHz frequency. Hence, the optimal value for L_3 is considered to be 13.3 *mm* (at constant $d_3 = 3.9\ mm$), which yields a notch band at center frequency 7.5 GHz.

To improve the overall performance of the antenna, various design parameters are examined to achieve the wide bandwidth with three-notch bands. The optimized design parameters of the proposed antenna structure are as follows: $W = 12\ mm, L = 19\ mm, d = 0.5\ mm, d_1 = 10.8\ mm, P_1 = 4.5\ mm, d_2 = 7.7\ mm, P_2 = 1\ mm, d_3 = 3.9\ mm, P_3 = 3.5\ mm, S = 0.5\ mm, L_g = 4.5\ mm, W_f = 1.9\ mm, L_f = 7.39\ mm$.

V. RESULTS AND DISCUSSION

A pair of fabricated prototypes of proposed antenna is presented with front and rear views in Fig. 14. The total length of

FIGURE 14. Prototypes of fabricated antenna.

TABLE 2. Simulation versus theoretical estimations for the notch bands.

$L_1 = d_1 + P_1$	15.3 mm
$L_2 = d_2 + P_2$	8.7 mm
$L_3 = 2 * P_3 + 2 * 2 * d_3 - (3 * 0.5)$	13.3 mm
1st notch band frequency (theory)	3.5 GHz 3.0 GHz
2nd notch band frequency (theory)	5.5 GHz 5.24 GHz
3rd notch band frequency (theory)	7.4 GHz 6.86 GHz

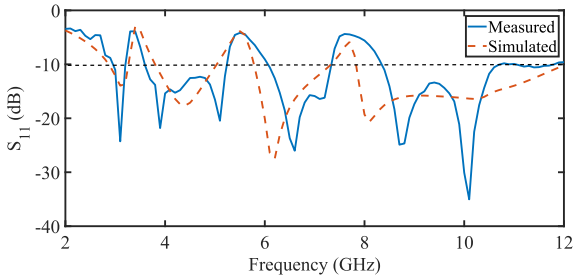

FIGURE 15. Reflection coefficient plot for the proposed antenna.

stubs and slots and corresponding simulated and theoretical estimated values are compared in Table 2. It can be observed that there is a slight deviation between them.

A. REFLECTION COEFFICIENT

Measured reflection coefficient result obtained from the Agilent N5230A PNA Network Analyzer is compared with simulated reflection coefficient result (HFSS software) as shown in Fig. 15. The reflection coefficient plot exhibits strong rejection in the WiMAX band from 3.3–3.8 GHz, WLAN band from 5.2–6.1 GHz and X band satellite communications from 7.3–8.2 GHz with a passband from 2.95–12 GHz. Measured reflection coefficient result is in good agreement with simulated reflection coefficient result. Slight deviation in higher frequencies might be due to substrate losses, measurement and fabrication errors.

B. GAIN AND RADIATION EFFICIENCY

This antenna exhibits stable radiation patterns throughout UWB range as demonstrated in Fig. 16. The radiation

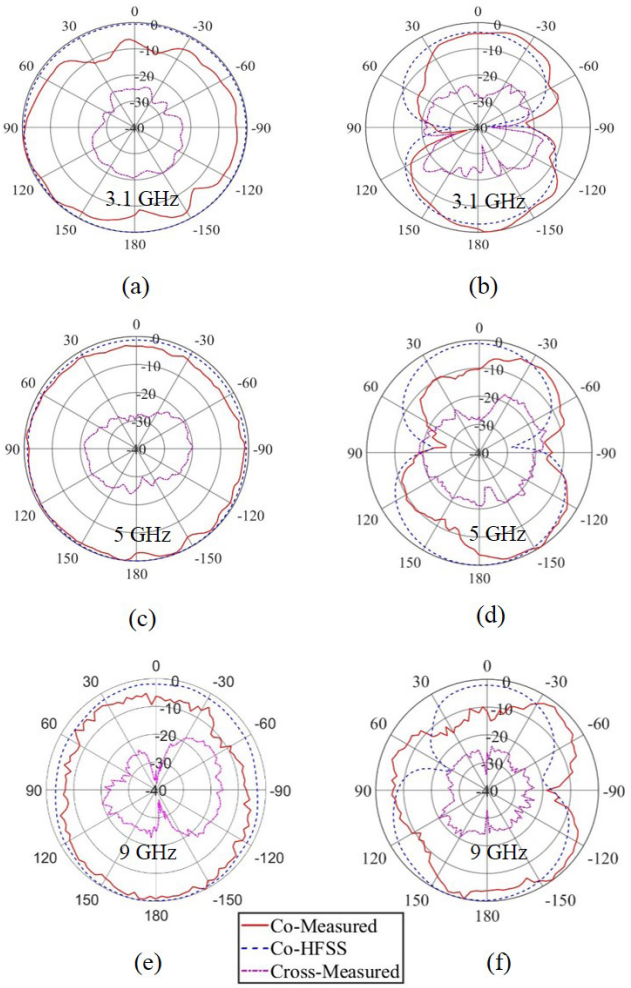

FIGURE 16. Comparison of measured and simulated radiation patterns of proposed antenna: (a, c, e) x-z plane, (b, d, f) y-z plane.

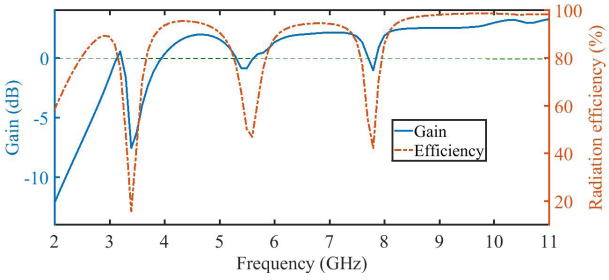

FIGURE 17. Gain and antenna radiation efficiency curves of the proposed antenna.

patterns are slightly distorted at higher frequencies due to the distortion in electric field distribution and the increased effect of harmonics of higher order modes. In Fig. 17, gain and efficiency values as a function of frequency are presented. However, the proposed antenna maintains stable gain at pass band frequencies. This antenna exhibits a maximum gain of 3.18 dB. A significant gain reduction (below 0 dB) is observed at notch band frequencies. Efficiency values are mainly depending on impedance matching between the

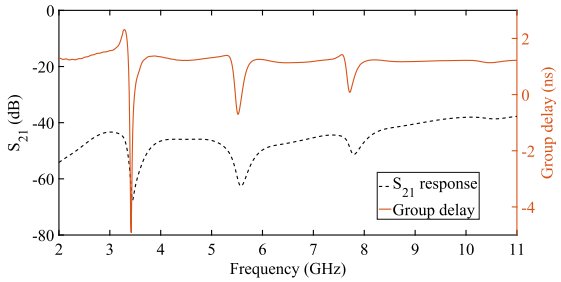

FIGURE 18. Group delay and S_{21} magnitude response of proposed antenna.

antenna element and feed line. Impedance mismatch leads to lower efficiency values. The proposed antenna structure exhibits adequate radiation efficiency in pass band frequencies and very low radiation efficiency in notch band frequencies. The pass band efficiency values are sufficient for satisfactory transmission and reception of signals.

C. GROUP DELAY

Low distortion is the primary requirement for UWB antennas. Time domain characteristics are used to evaluate the distortion present in the received signals [35]. Group delay is the essential characteristic of time domain analysis to measure the distortion. A constant group delay performance or linear magnitude response of S_{21} is indicative of low distortion. In Fig. 18, a constant group delay response is observed except in notch bands. Both these responses show the proposed antenna has very low distortion in the received signals in operating region and high in notch bands. To measure the group delay a gap of 30 *cm* is considered between the two antennas.

VI. CONCLUSION AND FUTURE SCOPE

A compact UWB antenna is designed and presented with triple band-notched characteristics to turn down the interference from existing WiMAX, WLAN and X band satellite communication channels. The simulated and measured −10 dB impedance bandwidths exhibit UWB frequency operation from 2.95–12 GHz with notch bands at WiMAX (3.3–3.8 GHz), WLAN (5.2–6.1 GHz), and X band satellite communications (7.3–8.2 GHz). Independent controllability of each notch band without disturbing UWB pass band is successfully achieved with this proposed antenna structure using L shaped stubs and CSRR slot. The proposed antenna can be a good choice for WBAN applications due to its compact dimensions, wide bandwidth and stable radiation patterns.

ACKNOWLEDGMENT

The authors sincerely thank Prof. K. J. Vinoy, Department of ECE, IISc Bangalore for allowing them to measure the radiation patterns using anechoic chamber.

REFERENCES

[1] M. N. Shakib, M. Moghavvemi, and W. N. L. B. W. Mahadi, "Design of a tri-band off-body antenna for WBAN communication," *IEEE Antennas Wireless Propag. Lett.*, vol. 16, pp. 210–213, 2017.

[2] S. Doddipalli, A. Kulkarni, P. Kaole, and A. Kothari, "Slotted substrate miniaturized ultra wideband antenna for WBAN applications," in *Proc. 9th Int. Conf. Comput., Commun. Netw. Technol. (ICCCNT)*, Bengaluru, India, Jul. 2018, pp. 1–4.
[3] J. C. Wang, E. G. Lim, M. Leach, Z. Wang, K. L. Man, and Y. Huang, "Review of wearable antennas for WBAN applications," *IAENG Int. J. Comput. Sci.*, vol. 43, no. 4, pp. 16–19, 2016.
[4] *Revision of Part 15 of the Commission's Rules Regarding Ultra-Wideband Transmission Systems*, FCC, Washington, DC, USA, 2002.
[5] S. Doddipalli, A. Kothari, and P. Peshwe, "A low profile ultrawide band monopole antenna for wearable applications," *Int. J. Antennas Propag.*, vol. 2017, Aug. 2017, Art. no. 7362431.
[6] M. Hayouni, F. Choubani, T. H. Vuong, and J. David, "Design and analysis of a compact printed UWB antenna using non uniform matching and half-wavelength circular slot," *Int. J. Electromagn. Appl.*, vol. 2, no. 6, pp. 145–150, 2012.
[7] M. Rahman and J.-D. Park, "The smallest form factor UWB antenna with quintuple rejection bands for IoT applications utilizing RSRR and RCSRR," *Sensors*, vol. 18, no. 3, p. 911, 2018.
[8] A. Rahman, M. T. Islam, M. J. Singh, S. Kibria, and M. Akhtaruzzaman, "Electromagnetic performances analysis of an ultra-wideband and flexible material antenna in microwave breast imaging: To implement a wearable medical bra," *Sci. Rep.*, vol. 6, Dec. 2016, Art. no. 38906.
[9] C.-M. Luo, J.-S. Hong, and H. Xiong, "A tri-band-notched UWB antenna with low mutual coupling between the band-notched structures," *Radioengineering*, vol. 22, no. 4, pp. 1233–1238, 2013.
[10] D. T. Nguyen, D. H. Lee, and H. C. Park, "Very compact printed triple band-notched UWB antenna with quarter-wavelength slots," *IEEE Antennas Wireless Propag. Lett.*, vol. 11, pp. 411–414, 2012.
[11] Y. Jin, J. Tak, and J. Choi, "Quadruple band-notched trapezoid UWB antenna with reduced gains in notch bands," *IEEE Antennas Wireless Propag. Lett.*, vol. 11, pp. 411–414, 2012.
[12] A. Yadav, S. Agrawal, and R. P. Yadav, and H. C. Park, "SRR and S-shape slot loaded triple band notched UWB antenna," *AEU-Int. J. Electron. Commun.*, vol. 79, pp. 192–198, Sep. 2017.
[13] A. Syed and R. W. Aldhaheri, "A new inset-fed UWB printed antenna with triple 3.5/5.5/7.5-GHz band-notched characteristics," *Turkish J. Elect. Eng. Comput. Sci.*, vol. 26, no. 3, pp. 1190–1201, 2018.
[14] M. Sharma, Y. K. Awasthi, and H. Singh, "Design of CPW-fed high rejection triple band-notch UWB antenna on silicon substrate with diverse wireless applications," *Prog. Electromagn. Res.*, vol. 74, pp. 19–30, 2017.
[15] I. B. Vendik, A. Rusakov, K. Kanjanasit, J. Hong, and D. Filonov, "Ultrawideband (UWB) planar antenna with single-, dual-, and triple-band notched characteristic based on electric ring resonator," *IEEE Antennas Wireless Propag. Lett.*, vol. 16, pp. 1597–1600, 2017.
[16] Y. Zehforoosh, M. Mohammadifar, and S. R. Ebadzadeh, "Designing four notched bands microstrip antenna for UWB applications, assessed by analytic hierarchy process method," *J. Microw., Optoelectron. Electromagn. Appl.*, vol. 16, no. 3, pp. 765–776, 2017.
[17] H. Choudhary *et al.*, "Design and analysis of triple band-notched microstrip UWB antenna," *Cogent Eng.*, vol. 3, no. 1, p. 1249603, 2016.
[18] E. K. I. Hamad and N. Mahmoud, "Compact tri-band notched characteristics UWB antenna for WiMAX, WLAN and X-band applications," *Adv. Electromagn.*, vol. 6, no. 2, pp. 53–58, 2017.
[19] K. Rayavaram, K. T. V. Reddy, and P. P. Kesari, "Compact UWB microstrip antenna with quadruple band-notched characteristics for short distance wireless tele-communication applications," *Int. J. Eng. Technol.*, vol. 7, no. 1, pp. 57–64, 2018.
[20] M. F. Habash, A. S. Tantawy, H. A. Atallah, and A. B. Abdel-Rahman, "Compact size triple notched-bands UWB antenna with sharp band-rejection characteristics at WiMAX and WLAN bands," *Adv. Electromagn.*, vol. 7, no. 3, pp. 99–103, 2018.
[21] H. A. Atallah, A. B. Abdel-Rahman, K. Yoshitomi, and R. K. Pokharel, "CPW-fed UWB antenna with sharp and high rejection multiple notched bands using stub loaded meander line resonator," *AEU-Int. J. Electron. Commun.*, vol. 83, pp. 22–31, Jan. 2018.
[22] S. R. Emadian and J. Ahmadi-Shokouh, "Study on frequency and time domain properties of novel triple band notched UWB antenna in indoor propagation channel," *Int. J. RF Microw. Comput.-Aided Eng.*, p. e21428, Aug. 2018.
[23] Z. Tang, R. Lian, and Y. Yin, "Differential-fed UWB patch antenna with triple band-notched characteristics," *Electron. Lett.*, vol. 51, no. 22, pp. 1728–1730, 2015.
[24] Y. Liu, Z. Chen, and S. Gong, "Triple band-notched aperture UWB antenna using hollow-cross-loop resonator," *Electron. Lett.*, vol. 50, no. 10, pp. 728–730, May 2014.
[25] J. Wang, Y. Yin, and X. Liu, "Triple band-notched ultra-wideband antenna using a pair of novel symmetrical resonators," *IET Microw., Antennas Propag.*, vol. 8, no. 14, pp. 1154–1160, 2014.
[26] F. Zhu *et al.*, "Multiple band-notched UWB antenna with band-rejected elements integrated in the feed line," *IEEE Trans. Antennas Propag.*, vol. 61, no. 8, pp. 3952–3960, Aug. 2013.
[27] M. Sharma, Y. K. Awasthi, H. Singh, R. Kumar, and S. Kumari, "Compact UWB antenna with high rejection triple band-notch characteristics for wireless applications," *Wireless Pers. Commun.*, vol. 97, no. 3, pp. 4129–4143, 2017.
[28] M. Sharma, Y. K. Awasthi, H. Singh, R. Kumar, and S. Kumari, "Compact printed high rejection triple band-notch UWB antenna with multiple wireless applications," *Eng. Sci. Technol., Int. J.*, vol. 19, no. 3, pp. 1626–1634, 2016.
[29] K. P. Ray and Y. Ranga, "Ultrawideband printed elliptical monopole antennas," *IEEE Trans. Antennas Propag.*, vol. 55, no. 4, pp. 1189–1192, Apr. 2007.
[30] M. S. Ellis, Z. Zhao, J. Wu, Z. Nie, and Q.-H. Liu, "A novel miniature band-notched wing-shaped monopole ultrawideband antenna," *IEEE Antennas Wireless Propag. Lett.*, vol. 12, pp. 1614–1617, 2013.
[31] Q. Wang and Y. Zhang, "Design of a compact UWB antenna with triple band-notched characteristics," *Int. J. Antennas Propag.*, vol. 2014, Jun. 2014, Art. no. 892765.
[32] L. Yang and K. Yoshitomi, "Design of a dual-band antenna with L-shaped stub," *IEICE Electron. Express*, vol. 8, no. 22, pp. 1887–1891, 2011.
[33] W.-H. Tu and K. Chang, "Compact microstrip bandstop filter using open stub and spurline," *IEEE Microw. Wireless Compon. Lett.*, vol. 15, no. 4, pp. 268–270, Apr. 2005.
[34] P. Sarkar, R. Ghatak, M. Pal, and D. R. Poddar, "Compact UWB bandpass filter with dual notch bands using open circuited stubs," *IEEE Microw. Wireless Compon. Lett.*, vol. 22, no. 9, pp. 453–455, Sep. 2012.
[35] W. Wiesbeck, G. Adamiuk, and C. Sturm, "Basic properties and design principles of UWB antennas," *Proc. IEEE*, vol. 97, no. 4, pp. 372–385, Feb. 2009.

Authors' photographs and biographies not available at the time of publication.